Published in Photosynthesis Research 79, issue 3, 233-248, 2004
which should be used for any reference to this work

Structural basis of redox signaling in photosynthesis: structure and function of ferredoxin:thioredoxin reductase and target enzymes

Shaodong Dai[2], Kenth Johansson[3], Myroslawa Miginiac-Maslow[4], Peter Schürmann[5] & Hans Eklund[1,*]

[1]*Department of Molecular Biosciences, SLU, Box 590, BMC, Husargatan 3 751 24 Uppsala, Sweden;* [2]*Integrated Department of Immunology, Howard Hughes Medical Institute, National Jewish Medical and Research Center & University of Colorado Health Sciences Center, 1400 Jackson St., K404, Denver, CO 80206, USA;* [3]*ESIL AFMB UMR 6098 CNRS-UI-UII, 163 Avenue de Luminy Case 925, 13009 Marseille, France;* [4]*Institut de Biotechnologie des Plantes, Bât. 630 Université Paris-Sud, 91405 Orsay Cedex, France;* [5]*Laboratoire de Biochimie Végétale, Université de Neuchâtel, Rue Emile Argand 11, 2007 Neuchâtel, Switzerland; *Author for correspondence (e-mail: hasse@xray.bmc.uu.se; fax: +46-18-536971)*

Key words: chloroplast enzymes, ferredoxin, fructose 1,6-bisphosphatase, glyceraldehyde 3-phosphate dehydrogenase, malate dehydrogenase, redox signalling, thioredoxin

Abstract

The role of the ferredoxin:thioredoxin system in the reversible light activation of chloroplast enzymes by thiol-disulfide interchange with thioredoxins is now well established. Recent fruitful collaboration between biochemists and structural biologists, reflected by the shared authorship of the paper, allowed to solve the structures of all of the components of the system, including several target enzymes, thus providing a structural basis for the elucidation of the activation mechanism at a molecular level. In the present Review, these structural data are analyzed in conjunction with the information that was obtained previously through biochemical and site-directed mutagenesis approaches. The unique 4Fe–4S cluster enzyme ferredoxin:thioredoxin reductase (FTR) uses photosynthetically reduced ferredoxin as an electron donor to reduce the disulfide bridge of different thioredoxin isoforms. Thioredoxins in turn reduce regulatory disulfides of various target enzymes. This process triggers conformational changes on these enzymes, allowing them to reach optimal activity. No common activation mechanism can be put forward for these enzymes, as every thioredoxin-regulated protein undergoes specific structural modifications. It is thus important to solve the structures of the individual target enzymes in order to fully understand the molecular mechanism of the redox regulation of each of them.

Abbreviations: FBPase – fructose-1,6-bisphosphatase; Fd – ferredoxin; FTR – ferredoxin:thioredoxin reductase; GAPDH – glyceraldehyde-3 phosphate dehydrogenase; NADP-MDH – NADP-malate dehydrogenase; NEM – N-ethyl maleimide; Trx – thioredoxin

Introduction

Photosynthetic organisms depend on light as a substrate providing the energy for the transformation of water and CO_2 into carbohydrates, which then serve as building blocks and energy source in the cellular metabolism. However, light is only available during the day and even during this period the light quantity as well as quality vary, for instance due to shading. Photosynthetic organisms have therefore developed a number of intricate regulatory mechanisms, which allow them to adapt to short-term as well as long-term changes in light conditions and to optimize their light-dependent metabolism. The signals provoking the adaptations are coming from the light perceived by photosynthetic pigments in the thylakoids and they are transmitted

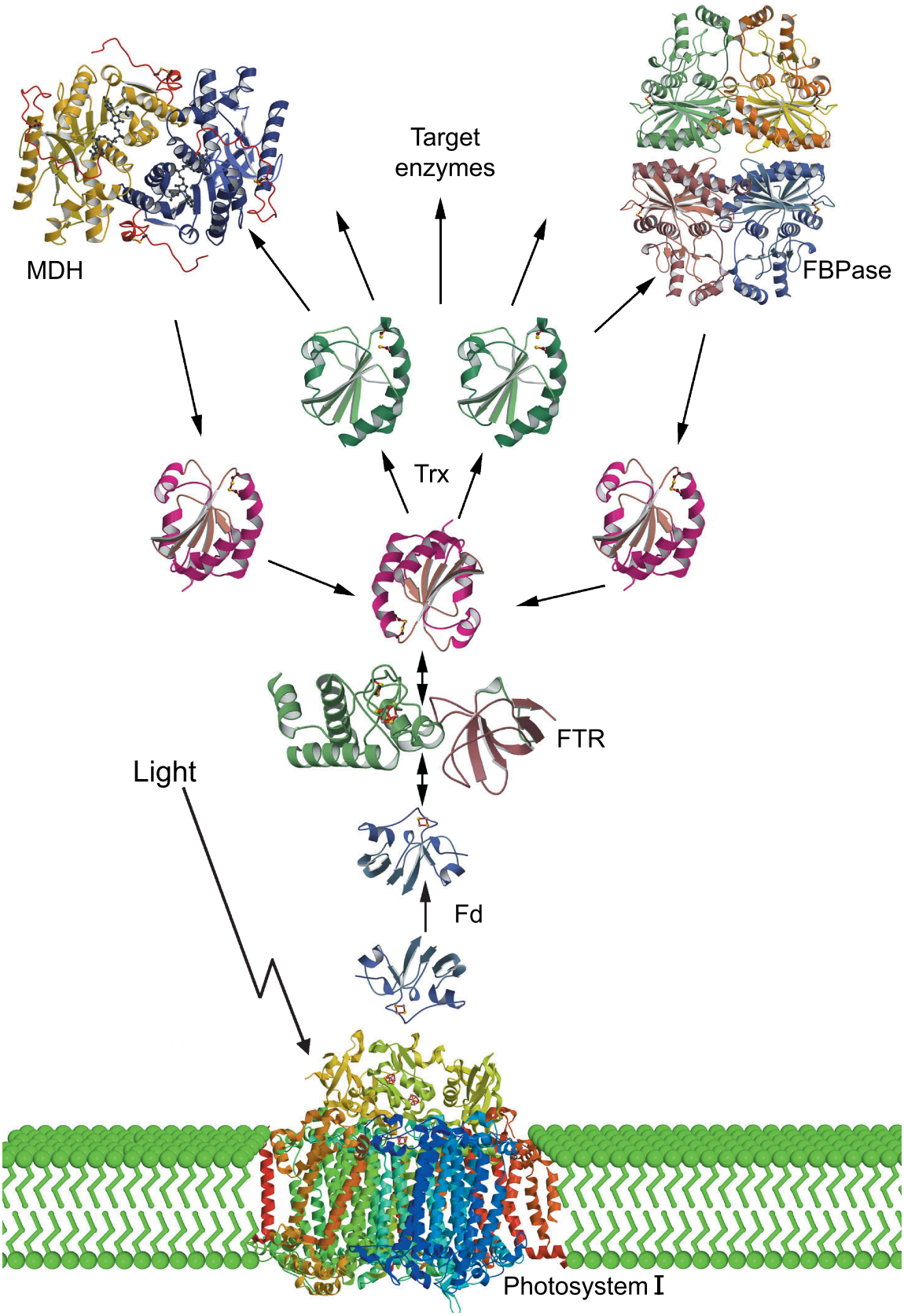

Figure 1

under various forms to different targets within the chloroplast.

One of these signals changing as a function of light is the redox potential in the stroma, which depends on the electron pressure built up by the light-driven electron transport. The mechanism, which senses the changes in redox potential, transforms this electronic signal into a biochemical signal in the form of disulfide/dithiol interchanges and transmits it to targets in the stroma, is known as the ferredoxin/thioredoxin system (Buchanan et al. 2002). This system is composed of three soluble chloroplast proteins, ferredoxin, ferredoxin:thioredoxin reductase (FTR) and thioredoxins (Schürmann 2003). In the light, ferredoxin is reduced by the photosynthetic electron transport and transmits electrons to various enzymes like ferredoxin:$NADP^+$ reductase, ferredoxin:nitrite reductase, sulfite reductase, glutamate synthase and FTR (Knaff 1996). The FTR, the central enzyme of the ferredoxin/thioredoxin regulatory system, transforms the electron signal into a disulfide/dithiol signal (Figure 1). This 'biochemical' signal is then transferred by thioredoxins through disulfide/dithiol interchanges to different target proteins, which, depending on their function in the metabolism, are activated or deactivated by reduction. This reduction is accompanied by a covalent modification of the target protein, which is entirely reversible upon reoxidation.

The activity of a number of chloroplast enzymes has been shown to be modified by reduction with thioredoxins. These enzymes are members of the reductive pentose phosphate cycle (FBPase, sedoheptulose 1,7-bisphosphatase, phosphoribulokinase, glyceraldehyde 3-phosphate dehydrogenase) and of the oxidative pentose phosphate cycle (glucose 6-phosphate dehydrogenase), or they are involved in activation of the ATP synthesis (ATP synthase) and of ribulose 1,5-bisphosphate carboxylase (Rubisco activase), and in the export of reducing equivalents through the 'malate valve' (NADP-malate dehydrogenase, NADP-MDH) or they participate in the metabolism of nitrogen, lipids and starch (Ruelland and Miginiac-Maslow 1999; Schürmann and Jacquot 2000; Schürmann and Buchanan 2001). Recent proteomic approaches revealed new putative targets and confirmed enzymes known to interact with thioredoxins (Motohashi et al. 2001; Balmer et al. 2003). A common feature of these enzymes is the presence of a redox-active disulfide bridge, which can be reduced by chloroplast thioredoxins (Schürmann and Jacquot 2000). This reduction proceeds via a transient, covalent heterodimer formation between thioredoxin and target enzyme. Such heterodimers have been demonstrated for phosphoribulokinase (Brandes et al. 1996), FBPase (Balmer and Schürmann 2001) and NADP-MDH (Goyer et al. 1999).

The regulatory aspects of the light-dependent chloroplast enzymes have been quite extensively studied (for reviews see Buchanan 1992; Wolosiuk et al. 1993; Miginiac-Maslow et al. 1997); however, structural information has not been available. During the past decade, the structures of the members of the ferredoxin/thioredoxin system and of two well-studied target enzymes have been solved. This has brought significant progress in the understanding of the system at the molecular level.

Reduced ferredoxin is produced in the light reaction of photosynthesis

In oxygenic photosynthesis of cyanobacteria and plants, PS I is one of the two pigment-containing reaction centers located in the thylakoid membrane (Barber and Andersson 1994). Upon illumination, the electron emitted from the excited P700* near the lumenal side of the thylakoid membrane is transferred across the membrane to the [4Fe–4S] clusters of subunit PsaC on the stromal side (Antonkine et al. 2003). The [4Fe–4S] clusters in turn reduce the [2Fe–2S] cluster of soluble ferredoxin. After being reduced by PsaC, ferredoxins can function as general soluble electron donors in the stroma, which initialize a number of important biological processes (Knaff 1996). A well-known function is the transfer of electrons to $NADP^+$ through the flavoenzyme ferredoxin:$NADP^+$ reductase. NADPH then provides the reducing power for the synthesis of carbohydrates.

Plant ferredoxins have a single [2Fe–2S] cluster, which operates at low redox potential, typically −400 mV. Several three-dimensional structures of plant-type ferredoxins are now available (Figure 1)

Figure 1 Light-induced enzyme regulation in chloroplasts through the FTR system. Upon illumination, the photosynthetic electron-transfer chain is initiated by the reduction of ferredoxin (Fd) by Photosystem I (PS I). Ferredoxin can then reduce FTR, which in turn reduces the chloroplast thioredoxins *m* and *f* (Trx). Finally, the thioredoxins activate (in one case deactivate) target enzymes, here exemplified by malate dehydrogenase (MDH) and fructose 1,6-bisphosphatase (FBPase), thereby changing the metabolism to anabolic pathways. In the figure, the oxidized thioredoxins are in red and reduced thioredoxins in green.

and share the same fold with a five-stranded β-sheet, 2-3 α-helices and a long loop containing three or four cysteine ligands to the iron atoms. Inorganic sulfide ions and cysteine residues tetrahedrally coordinate the two irons. All plant-type ferredoxins possess a fully conserved cluster-binding sequence motif $CX_4CX_2CX_{22-33}C$. The iron–sulfur clusters of all are located towards the outer edge of the molecule in the loop.

Thioredoxin *f* (Trx-*f*) and *m* (Trx-*m*)

Thioredoxins are small ubiquitous redox proteins with a number of important cellular functions (Powis and Montfort 2001). Only two thioredoxins have been implicated in the ferredoxin:thioredoxin system, Trx-*f* and Trx-*m* and they were distinguished and named according to their target enzyme specificity (Schürmann and Jacquot 2000). Whereas Trx-*f* displayed a high specificity towards chloroplast FBPase, Trx-*m* interacted very efficiently with NADP-MDH. A comparison of the efficiency of the two thioredoxins in reducing carbon metabolism enzymes suggests however, that Trx-*f* functions primarily in enzyme activation and Trx-*m* in enzyme deactivation (Schürmann 2003).

Trx-*f* and Trx-*m* are α/β-proteins which have a central five-stranded β-sheet surrounded by four helices with a redox-active disulfide at the N-terminus of α2 (Capitani et al. 2000) (Figure 1). In addition, Trx-*f* has an extra N-terminal helix. Their overall structure is similar in spite of the low sequence similarities; the primary structures of the two chloroplast thioredoxins are only 30% identical. Trx-*f* has a substantially different distribution of polar, charged and hydrophobic residues around the active site with respect to Trx-*m*. The active site of Trx-*f* is surrounded by a number of positive charges which may be involved in orienting Trx-*f* correctly when it interacts with its target proteins. A difference between Trx-*f* and Trx-*m* is the presence of a third cysteine, which is conserved in all Trx-*f*s. In the crystal structure, this

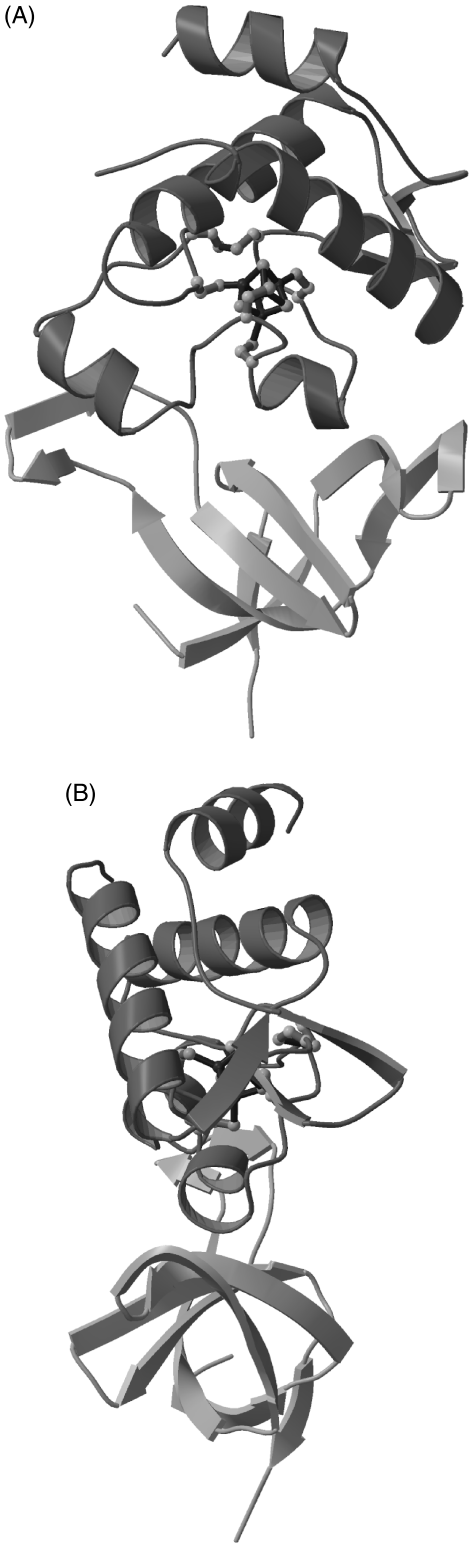

Figure 2 The FTR heterodimer. (A) The catalytic subunit (dark gray) has an overall α-helical structure with loops between the helices containing the iron–sulfur ligands and redox-active cysteines. The variable subunit (light gray) is heart shaped with the β-barrel forming the main body and with two loops forming the upper, outer parts of the heart. (B) FTR is an unusually thin molecule, a concave disk with dimensions 40×50 Å but only 10 Å across the center of the molecule where the iron–sulfur cluster center is located.

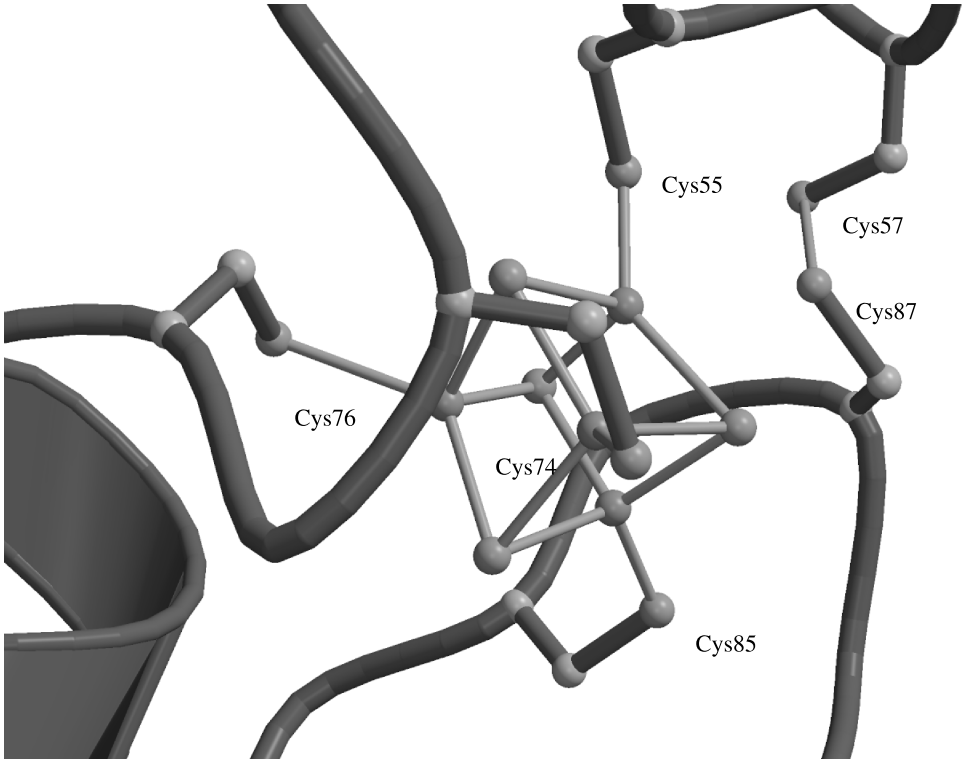

Figure 3 The active site of FTR. The irons of the iron–sulfur center are coordinated by cysteines 55, 74, 76 and 85. The active site disulfide bridge is between residues 57 and 87 (to the right). Cys 87 is in van der Waals contact with the iron center.

Cys73 is exposed on the surface, 9.7 Å away from the accessible active-site Cys46 (Capitani et al. 2000). Mutagenesis studies show that this residue may participate in the interactions with the target enzyme (del Val et al. 1999).

FTR

FTR transduces the general redox signal from ferredoxin to thioredoxins. It is an iron–sulfur protein with a redox-active disulfide bridge that utilizes a [4Fe–4S] cluster to mediate electron transfer from the one-electron donor, the $[2Fe–2S]^{2+}$ cluster of ferredoxin, to the two-electron acceptor, the disulfide bridge of thioredoxin. Reduced thioredoxin then transfers the electrons to target enzymes via thiol/disulfide interchange reactions. It reduces the chloroplastic *f*- and *m*-type thioredoxins.

Most biochemical investigations have been done on the spinach enzyme, whereas the only three-dimensional structure of FTR is from the cyanobacterium *Synechocystis* sp. PCC6803 (Dai et al. 2000). This FTR shows no functional difference to the spinach enzyme but it is significantly more stable (Schwendtmayer et al. 1998). Sequences for the FTRs are available from several species which indicates that the cyanobacterium FTR-structure is a good prototype for all FTRs. FTR is a heterodimer composed of a 13 kDa catalytic subunit with conserved sequence between species and a variable subunit of similar or smaller size. The catalytic subunit contains a redox active disulfide and a [4Fe–4S]-center.

The FTR-variable subunit is an open β-barrel structure, which contains five antiparallel strands (Figure 2). The catalytic subunit has an α-helical structure containing five helices. The N-terminal half of the subunit, together with the C-terminal helix, forms an α-helical cap on top of the iron–sulfur center while the intervening 40 residues contain all the iron ligands and redox active cysteines. This part contains two additional short helices and intervening loops. The helical structure of the catalytic subunit of FTR distinguishes it from most other [4Fe–4S] proteins.

The FTR heterodimer is an unusually thin molecule, a concave disk with dimensions 40 Å × 50 Å with only 10 Å across the center of the molecule where the iron–sulfur center is located (Figure 2B). The in-

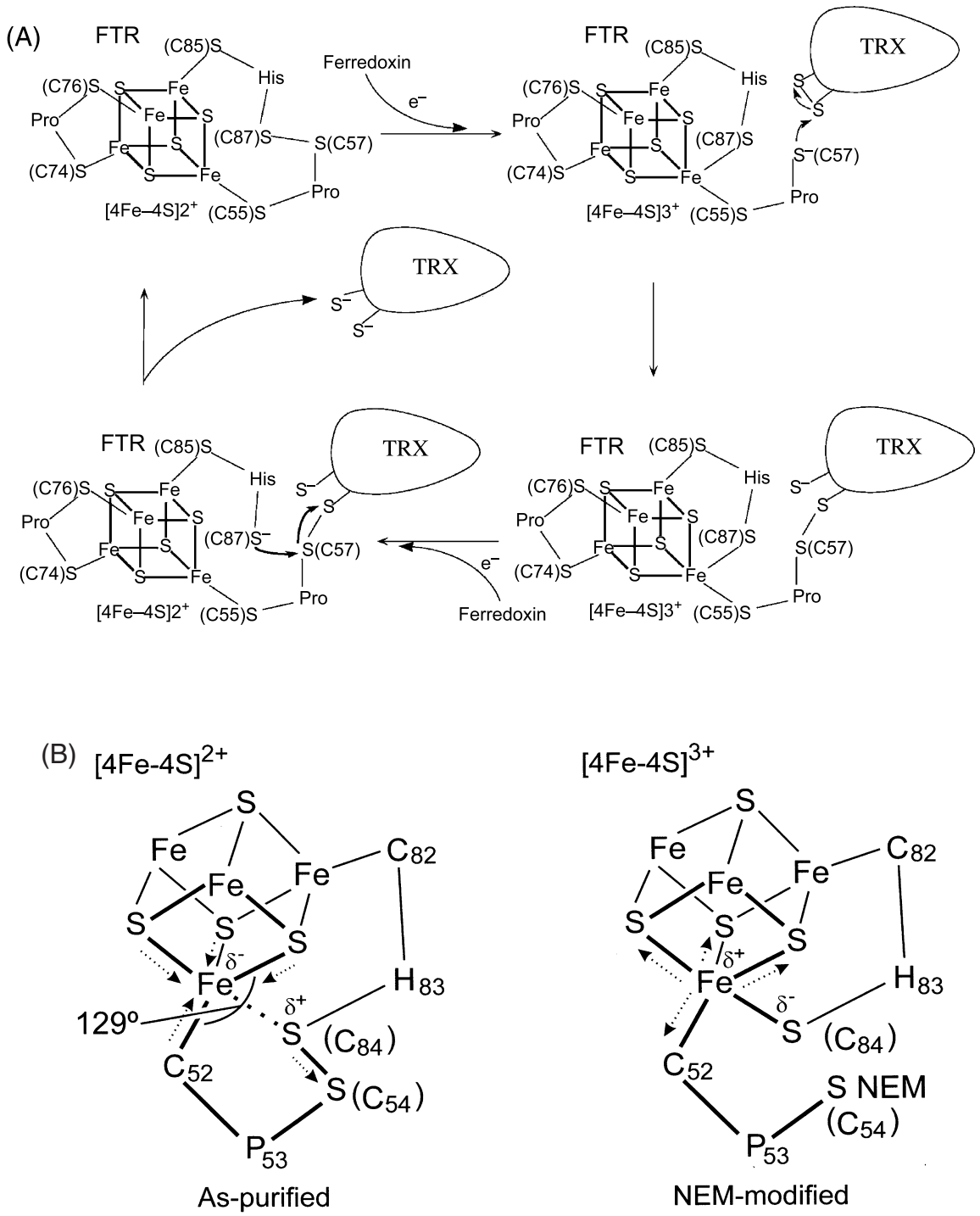

Figure 4 (A) Suggested mechanism of action (Dai et al. 2000), in which Cys87 coordinates the iron in the intermediate stage. The tight interaction by Cys87 with one of the irons of the cluster in the FTR structure implicates that Cys87 coordinates the iron in a five-coordinated cluster. (B) The FTR mechanism has been explained in a donor–acceptor approach involving the active-site disulfide and the unique Fe site of the [4Fe–4S] cluster (Jameson et al. 2003). Partial bonding of the disulfide to the unique iron in the resting state of the cluster promotes charge build-up on that iron, making it an electron donor with increased ferrous character and polarizes the S–S bond making the interactive sulfur an electron acceptor (left panel). The one-electron reduced state is modeled by the NEM-modified form (right panel). The binding of an additional cysteine to the unique Fe reverses the donor–acceptor properties, and charge is drawn away from the iron. (The residue numbers are according to the spinach sequence.) Reprinted with permission from Jameson et al. (2003) © American Chemical Society.

teractions between the catalytic and variable chains involve the very thin center of the molecule where only a small hydrophobic core is formed. Instead, most of the interactions between the subunits occur between charged and polar residues forming hydrogen bonds.

The iron–sulfur center and active-site disulfide bridge are both located in the catalytic subunit. The irons of the iron–sulfur center (Figure 3) are coordinated by cysteines 55, 74, 76 and 85. All iron ligands are located in short sequence motifs CXC, which constitutes a unique arrangement with the fingerprint $CPCX_{16}CPCX_8CHC$. Both cysteines in the central CPC motif are ligands to the iron–sulfur center while in the other two motifs the liganding cysteines are connected to the redox-active cysteines in one CPC and one CHC motif where the second cysteines in these motifs are forming the disulfide bridge. The active-site disulfide bridge is in van der Waals contact with the iron center, primarily the sulfur atom of Cys87 contacts the iron atom bound by Cys55 (Figure 3). The sulfur atom of Cys87 is at 3.1 Å distance to the iron bound by Cys55 and to the sulfur atom of this cysteine. The closest sulfide ion of the cluster is 3.4 Å away from Cys87. Replacement of Cys87 (Cys84 in the spinach FTR) by Ser completely destabilizes the Fe–S center rendering the protein labile and impossible to purify (Manieri et al. 2003). The iron center is surrounded exclusively by hydrophobic residues all coming from the catalytic subunit.

Redox states of FTR

The iron center of FTR has some unusual properties. Spectroscopic investigations have shown that the stable redox state of the [4Fe–4S] cluster is 2+. Reduction of the center by one electron from ferredoxin results in an oxidized $[4Fe–4S]^{3+}$ cluster where the electron from ferredoxin plus one electron from the iron center have reduced the disulfide of FTR. However, in the reduced disulfide, only one of the cysteines, Cys57 is a free thiol whereas the other cysteine, Cys87, is coordinated to the iron center. Thus, the cluster stabilizes the one-electron-reduced reaction intermediate. An additional electron from a second ferredoxin is necessary to reduce the iron center back to 2+ and free Cys87.

Two configurations for the one-electron-reduced intermediate have been suggested; either a disulfide bridge with a sulfide ion in the cluster or a five-coordinated iron where the fifth ligand should be Cys87. Staples et al. (1998) favored the intermediate forming a disulfide with a sulfide ion of the cluster because the sulfide ion should be a good nucleophile for the reaction. Dai et al. (2000) instead favored that Cys87 in the intermediate stage coordinates the iron (Figure 4A) because of its close connections with one of the irons of the cluster in the FTR and redox properties of similar five-coordinated model compounds. Recent Mössbauer studies also appear to favor such a five-coordinated intermediate (Figure 4B) (Jameson et al. 2003).

Spectroscopic studies demonstrated that alkylation of one of the active-site cysteines with N-ethylmaleimide resulted in similar spectroscopic signals as those obtained when native FTR was reduced to a one-electron-reduced FTR reaction intermediate (Staples et al. 1998). This species is thus a good model for the intermediate and has been used in further studies.

Mechanism of action of FTR

The reduction of a disulfide is a two-electron process whereas ferredoxin is a one-electron carrier. The initial electron delivered from a ferredoxin molecule can be transferred via the iron–sulfur center directly to the disulfide that is in close contact with one iron atom of the cluster. Thereby, the intermediate with a free Cys57 and with Cys87 coordinated to the oxidized iron-center is formed. Cys57 at the molecular surface of FTR can then act as a nucleophile attacking the thioredoxin disulfide in the first step of the reaction. His86 and Arg58 are very close to the disulfide bridge (3.9 and 5.6 Å, respectively) and might increase the nucleophilicity of the cysteine.

In analogy with known mechanisms, the reduction of thioredoxin proceeds via a mixed disulfide between thioredoxin and FTR (Staples et al. 1996, 1998). Such an intermediate complex would cover one of the sides of the flat FTR molecule and the second electron for the reduction should be delivered by the next incoming ferredoxin, which has to dock on the opposite side of the flat disk-like heterodimer. The thin FTR molecule seems ideally suited for electron transfer between ferredoxin and thioredoxin.

A thioredoxin–FTR complex was originally modeled using the cyanobacterial *Anabaena* thioredoxin (Saarinen et al. 1995) by forming a mixed disulfide with the exposed cysteine covalently bound to Cys57 of FTR. Cys57 lies in a concave face of FTR

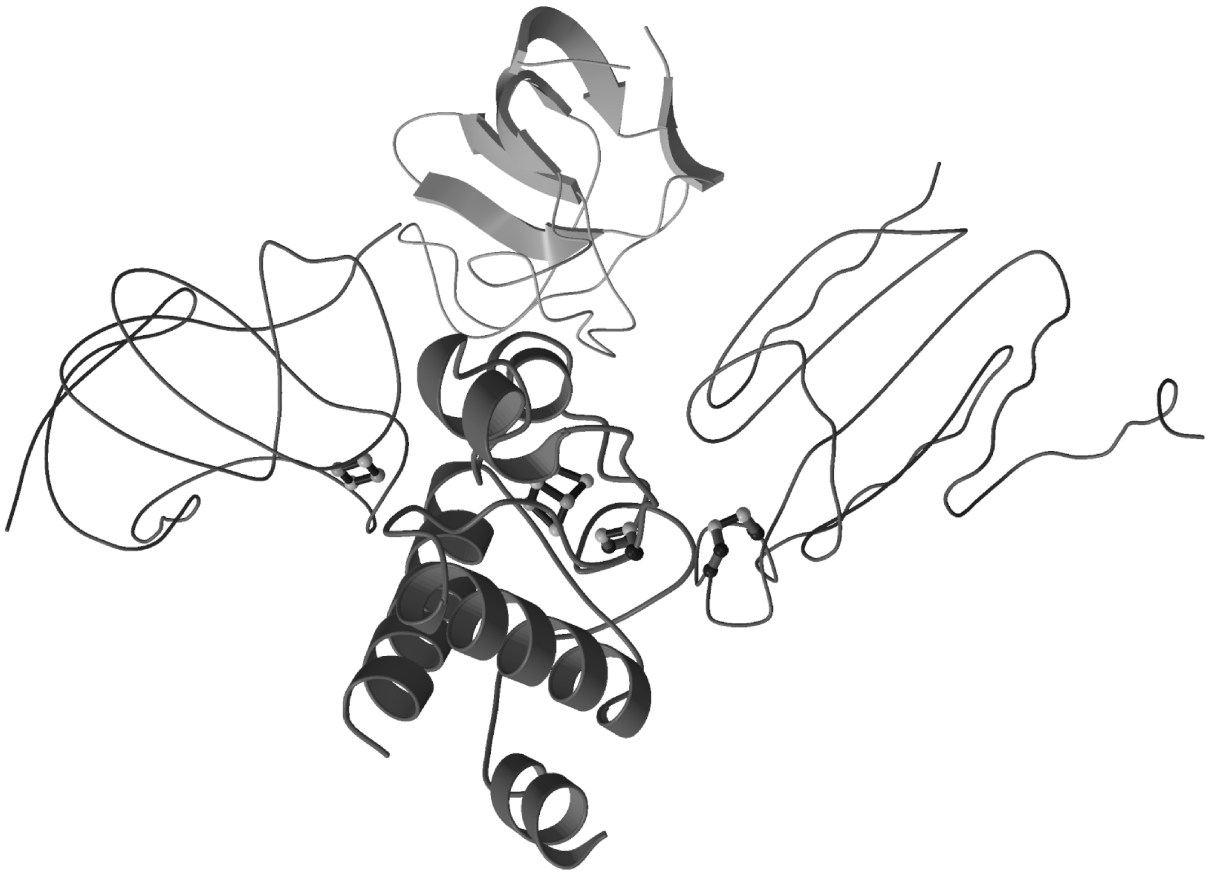

Figure 5 Modeling of the electron-transport chain from ferredoxin to thioredoxin. The disc-shaped structure of the FTR allows docking of a ferredoxin on one side of the molecule (to the left), while thioredoxin binds to the other side and forms a heterodisulfide with the enzyme (to the right). This intermediate can be reduced by an electron from a second ferredoxin molecule. The iron–sulfur centers and disulfide bridges are shown in ball- and stick-representation.

that can give favorable interactions to the docked thioredoxin. The concave shape of the opposite side is complementary to ferredoxin, and ferredoxins from different organisms could be docked to FTR. Positively charged residues of FTR could be matched with negatively charged residues of ferredoxin. The docking of ferredoxin to FTR is roughly consistent with chemical modification studies of acidic residues where binding to FTR inhibits modification of ferredoxin residues Asp34, Asp65, Glu92, Glu93, Glu94 and the C-terminus (De Pascalis et al. 1994). These residues form a surface around the [2Fe–2S] cluster directed towards FTR in the model.

Pro75 connects the iron–sulfur ligands on the ferredoxin side of the disk-formed FTR molecule in a CPC motif. The main chain of this motif is exposed towards the ferredoxin side and docking of a ferredoxin to this site should give a short through-bond electron transfer route from the bound ferredoxin to the iron–sulfur center. The short distance through the enzyme from the ferredoxin docking site through the iron–sulfur center to the closely associated Cys87 of the active site disulfide seem ideally suited for its purpose.

Some hydrophobic residues around the Fe–S cluster might also be involved in this interaction. The thioredoxin interaction area is different and contains more hydrophobic residues and three histidines one of them very close to the active site. Glu84 about 12 Å away is the only negatively charged residue not too far from the disulfide in FTR, which may fit with a positively charged residue in thioredoxin.

The second electron delivered by a new ferredoxin molecule to the ferredoxin-binding site reduces the iron–sulfur center back to its original 2+ oxidation state while Cys87 becomes a nucleophilic thiol that can attack the heterodisulfide bridge between FTR

and thioredoxin and thereby release the fully reduced thioredoxin. Such a mechanism is entirely compatible with the disk-shaped structure of FTR, which would allow docking of a second ferredoxin molecule on one side of the molecule, while thioredoxin is bound to the other side via the intermolecular disulfide bridge (Figure 5).

All known biological disulfide reductions except the one by FTR and homologues are catalyzed by flavoproteins or by thiol–disulfide exchange reactions (Williams 1992). The FTR is completely different from the bacterial, plant and mammalian thioredoxin reductases which are flavoproteins reduced by NADPH (Williams 1992; Dai et al. 1996; Jacquot et al. 1997). The unique property of the FTR iron–sulfur center to be able to cleave a disulfide does not appear to be due to an unusual geometry of the iron center since the iron–sulfur cluster is very similar to other [4Fe–4S] clusters. The environment of the iron–sulfur cluster is neither exceptional having, on average, one hydrogen bond per liganding cysteine and otherwise a surrounding hydrophobic environment. The only unusual feature of the iron center is the close proximity of the active-site disulfide bridge.

Mössbauer investigations have demonstrated that a partial bonding of the disulfide in the resting state to the iron–sulfur cluster promotes charge buildup on the close iron (Figure 4B) making it an electron donor with increased ferrous character (Jameson et al. 2003). The system is therefore primed and ready to accept an electron from ferredoxin to break the disulfide bond (Figure 4B). The binding of an additional cysteine to the iron makes it more ferric and charge is drawn away from the iron.

Redox-potential measurements on the components of the ferredoxin/thioredoxin system have shown that there is sufficient thermodynamic driving force to transfer electrons from ferredoxin to the Trxs. The potential difference between ferredoxin ($E_{m,7.0} = -420\,mV$), FTR ($-320\,mV$) and Trxs *m* or *f* (-300 resp. $-290\,mV$) are large enough to keep both chloroplast Trxs essentially reduced in the light (Hirasawa et al. 1999).

FTR from different species

The sequences of the catalytic subunits of FTR are highly conserved among all known species. All ligands to the iron–sulfur center and the surrounding hydrophobic residues are conserved as well as the active-site cysteines. Several residues in the catalytic subunit, which participate in subunit interactions, are conserved.

The surfaces on both sides of the molecule that should form the main interaction area with ferredoxin on one side and thioredoxin at the other are highly conserved. The ferredoxin interaction area contains three positively charged residues at about 10 Å from the cluster. They might be responsible for the correct orientation of the negatively charged ferredoxin when it is docked. Some hydrophobic residues around the Fe–S cluster might also be involved in this interaction. The thioredoxin interaction area is different and contains more hydrophobic residues and three histidines, one of them very close to the active site. Glu84 about 12 Å away is the only negatively charged residue not too far from the disulfide in FTR, which may fit with a positively charged residue in thioredoxin.

The plant enzymes have extensions in the N-terminal, but besides this, few differences exist in chain length in the variable chain. The long N-terminus in the spinach variable chain has been shown with deletion mutants *in vitro* (16 or 24 residues deleted respectively) not to be important for catalysis. This is consistent with the position of the N-terminus in *Synechocystis* FTR on the side farthest away from the catalytic subunit. However, removal of the extended N-terminus of the spinach FTR has a beneficial effect on the structure of the protein, rendering it significantly more stable (Manieri et al. 2003).

All conserved residues in the variable chain are either internal or glycines that are conserved for structural reasons and residues in the interaction area with the catalytic subunit. Residues in a long loop form most of these interactions but also involve a few residues at the ends of the other strands. Among the conserved residues are those, which make hydrogen bonds to the catalytic subunit.

Target enzymes

Since redox regulation by the ferredoxin/thioredoxin system proceeds through thiol–disulfide interchange with thioredoxins, a regulatory disulfide, which can be reduced by thioredoxin, has to be present in the target enzymes. For several target enzymes, involved in the photosynthetic carbon assimilation, the regulatory cysteines have been located in the primary structure and the principal activator thioredoxin determined (Schürmann and Jacquot 2000; Schürmann

and Buchanan 2001). Structural information is available for two of the target enzymes, FBPase and NADP-MDH (Villeret et al. 1995; Carr et al. 1999; Chiadmi et al. 1999; Johansson et al. 1999) as well as for the constitutively active A-form of the glyceraldehyde phosphate dehydrogenase (GAPDH) (Fermani et al. 2001).

The combination of biochemical and structural approaches has proved to be particularly useful to get an insight into the intramolecular events leading to the activation of these enzymes. The foundation for light activation is emerging as we are beginning to grasp the underlying processes taking place during the final activating steps of the redox cascade.

NADP-MDH

Among the target enzymes, one of the most complex activation mechanisms is displayed by NADP-MDH (EC.1.1.1.82) that reduces oxaloacetate into malate. NADP-MDH is found in chloroplasts of C_3 and C_4 plants. In C_3 plants, it is not directly implicated in carbon fixation, but functions in a shuttle mechanism exporting excess of reducing equivalents to the cytosol. In C_4 plants, in which the primary CO_2-fixation product is oxaloacetate, the mesophyll chloroplast NADP-MDH belongs to the photosynthetic machinery. Malate is exported to the bundle sheath chloroplasts where it is reoxidized and decarboxylated by NADP-malic enzyme, generating NADPH and CO_2 for the operation of the Calvin cycle (Hatch 1987). As this CO_2 trapping and concentrating mechanism is highly energy dependent, its strict control is very important. For the homodimeric NADP-MDH, this control is accomplished by the thioredoxin-mediated reversible breaking of two different regulatory disulfides per monomer: an N-terminal one, linking Cys24 and Cys29 (Sorghum numbering) and a C-terminal one, linking Cys365 and Cys377. Both disulfides are located in sequence extensions specific for the redox-regulated NADP-dependent isoform and missing in the constitutively active NAD-dependent isoforms.

Both disulfides are reduced rapidly (Miginiac-Maslow et al. 1990). However, site-directed mutagenesis studies showed that their roles in activation are quite different. Substitution of the N-terminal cysteines results in an acceleration of the activation rate (Issakidis et al. 1992), suggesting that a rate-limiting slow conformational change follows the breaking of the N-terminal disulfide. Substitution of the C-terminal cysteines confers some activity on the oxidized protein, with a very poor Km for oxaloacetate but unchanged activation rate (Issakidis et al. 1994). This mutation makes the catalytic histidine accessible to specific derivatizing reagents (Lemaire et al. 1994) indicating that the breaking of the C-terminal disulfide gives access to the active site (Issakidis et al. 1996). Additional mutations shed some light on the mechanism whereby the active site is blocked in the oxidized enzyme. Substitution of the penultimate C-terminal Glu for Gln, or deletion of the two C-terminal residues, combined with the mutation of the N-terminal disulfide, yields a fully active oxidized protein (Ruelland et al. 1998), suggesting the implication of the negatively charged Glu in blocking the active site. The positively charged partner of this Glu was shown to be Arg204, a residue involved in binding oxaloacetate in all malate dehydrogenases (Schepens et al. 2000b), indicating a direct interaction of the C-terminus with active-site residues.

An additional redox effect modulates the activity of NADP-MDH. The activation is inhibited by $NADP^+$, but not by NAD^+. When the cofactor specificity was changed from NADPH to NADH (Schepens et al. 2000a), the inhibitory effect was shifted from $NADP^+$ to NAD^+, demonstrating that it occurs through the binding of the oxidized cofactor to the active site. No inhibition was observed with activated WT protein, nor with proteins mutated either on the penultimate Glu, or on the C-terminal disulfide.

The determination of the three-dimensional structure of oxidized NADP-MDH from sorghum (Johansson et al. 1999) and *Flaveria* (Carr et al. 1999) provided structural support for the biochemical observations, yielding convergent and fully coherent results (Figure 6). The two subunits of NADP-MDH are oriented head-to-tail. The N-terminal extensions are located at the subunit interface area, making hydrophobic interactions with both monomers, thus rigidifying the structure of the dimer. Disulfide reduction probably loosens the interaction, conferring on the catalytic domain the flexibility necessary for optimal catalytic efficiency. The C-terminal extensions are positioned on the outside and each extension is pulled back by the C-terminal disulfide towards the active site where the two most C-terminal residues occupy the place of oxaloacetate, acting as internal inhibitors, a process termed ‘intrasteric inhibition’ (Kobe and Kemp 1999). In the *Sorghum* structure, the penultimate Glu388 interacts with Arg204. In the *Flaveria*

structure, a molecule of $NADP^+$ is present and its positively charged nicotinamide ring interacts with Glu388 and anchors it more tightly to the active site. This feature explains why, in the presence of $NADP^+$, the activation is slowed down and why the inhibitory effect of the oxidized cofactor is suppressed when the two most C-terminal residues are deleted or displaced by the reduction of the C-terminal disulfide. The three-dimensional structure also reveals that Cys207, proposed to be involved in the formation of a transient disulfide during activation (Ruelland et al. 1997), is located close to the subunit interface and to the N-terminal Cys24 of the neighboring subunit. Thus, if this transient disulfide is formed, it must cross-link the two subunits. An inter-subunit disulfide has been identified on non-reducing SDS-PAGE on a mutated MDH (Goyer et al. 2001). Whether it is physiological or due to the mutation of Cys29, remains to be determined.

Attempts to crystallize the active form of the enzyme failed so far. However, two-dimensional proton NMR experiments, performed with a monomeric N-terminal truncated NADP-MDH, revealed that the C-terminal extension (a 15-amino-acid stretch spanning from Ala375 to Val389) became mobile in the activated form (Krimm et al. 1999). This result could be further confirmed and extended with N^{15} labeled, dimeric, full-length NADP-MDH (manuscript in preparation). This indicates that upon reduction of the C-terminal disulfide, the C-terminal extension is expelled from the active site and becomes flexible. The Cys365 member of this disulfide belongs to the core part of the molecule, thus, when the disulfide forms again upon oxidation, it should be able to pull back the extension into the active site.

A detailed review of the regulatory properties of NADP-MDH has been published recently (Miginiac-Maslow and Lancelin 2002). The major redox-regulatory mechanism of NADP-MDH is obviously the auto-inhibition by the C-terminal extension. The events linked to the reduction of the N-terminal disulfide, although not yet fully understood, superimpose a kinetic fine-tuning on this regulation. Another fine-tuning is provided by the Trx redox state. Indeed, the redox potentials of the two regulatory disulfides of NADP-MDH are not identical: the N-terminal disulfide is isopotential with Trx, while the C-terminal disulfide is more electronegative, and would require an excess of reduced Trx to be reduced (Hirasawa et al. 2000). This supplementary degree of sophistication is an evolutionary trait proper to higher plants. In this respect, it can be noted that NADP-MDH of the green alga *Chlamydomonas* has no cysteines in its N-terminal extension (Gomez et al. 2002). Preliminary experiments showed that this MDH has faster activation kinetics, without the lag phase specific for the higher plant enzymes (Lemaire et al. 2003). The NADP-dependent, light-activated enzyme does neither exist in prokaryotes, nor in red algae or diatoms (Ocheretina et al. 2000). As its main function is the export of reducing equivalents from the chloroplast to the cytosol, this seems to constitute an adaptative mechanism in most photosynthetic eukaryotes, especially C_4-type plants.

It was long considered as a dogma that the activation of NADP-MDH exhibits little specificity towards a given Trx isoform. Therefore, MDH activation was used as a standard test in Trx purification procedures. With the development of genome sequencing projects, new chloroplast Trxs could be identified (Meyer et al. 2002; Lemaire et al. 2003). Some of them were shown to be unable to activate NADP-MDH while being active donors of reducing equivalents to peroxiredoxins (Collin et al. 2003; Lemaire et al. 2003). Thus, the very conserved Trx active-site WCGPC is not the only determinant of the interaction of Trx with NADP-MDH; some more specific features have still to be defined.

Fructose-1,6-bisphosphatase

Chloroplastic FBPase (EC 3.1.3.11) belongs to the Calvin-cycle enzymes and catalyzes the hydrolysis of fructose-1,6-bisphosphate into fructose-6-phosphate. It has long been recognized as a regulatory step of the photosynthetic CO_2-assimilation pathway and as being activated in the light by the ferredoxin/thioredoxin cascade (Schürmann and Jacquot 2000).

However, thioredoxin is not the only modulator of its activity, several other factors linked to light induced changes in the chloroplast stroma increase its catalytic efficiency: (a) raise of the stromal pH from 7 in the dark to 8 in the light, close to the optimal pH for catalysis; (b) increase in Mg concentration, and (c) build-up of the substrate concentration, which has a stabilizing effect on the enzyme. A long-time puzzling observation was that *in vitro*, the activation by reduced thioredoxin could be mimicked by increasing Mg concentration in the reaction medium.

FBPases exist also in the cytosol. These cytosolic isoforms are redox-independent, but are instead allosterically regulated by AMP. Compared to these

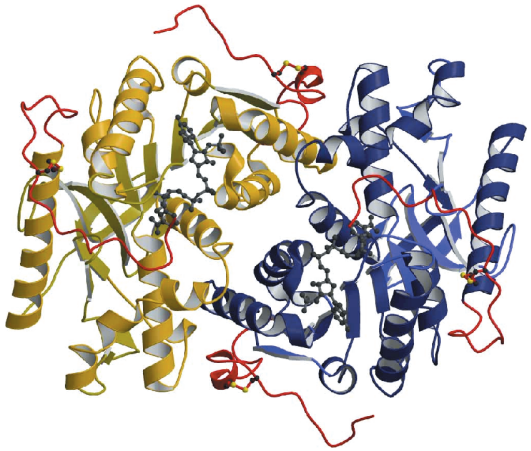

Figure 6

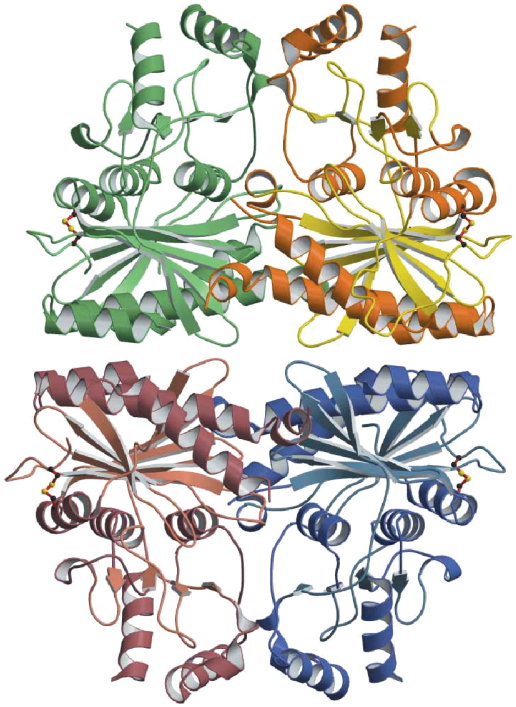

Figure 7

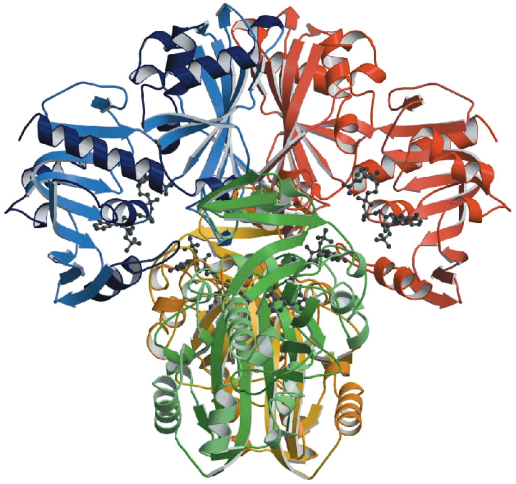

Figure 8

isoforms, the chloroplastic redox-regulated FBPases bear an insertion of 14–19 residues in their amino-acid sequence, featuring three conserved cysteine residues. Site-directed mutagenesis of these cysteines showed that one of them, namely Cys153, was involved in a regulatory disulfide with either Cys175 or Cys178 (pea numbering). Indeed, a fully active, redox-independent enzyme could be obtained either by mutating Cys153 alone, or by mutating either Cys173 or Cys178 (Jacquot et al. 1997). The definite answer was provided by structural approaches. When the three-dimensional structure of the tetrameric oxidized pea FBPase was determined by X-ray crystallography (Figure 7), a disulfide linking Cys153 and Cys173 could be localized (Chiadmi et al. 1999), suggesting that the Cys153–Cys178 disulfide was formed only when Cys173 was mutated, due to its proximity to the latter Cys. The analyses of a corresponding spinach mutant FBPase by CD spectroscopy and SH-titrations strongly support this hypothesis (Balmer et al. 2001). A structure of spinach chloroplast FBPase had been published previously (Villeret et al. 1995). In this structure, no disulfide was visible and its general features suggested that it represented a reduced (activated) form of the enzyme. This allows comparing both structures and identifying the modifications induced by reducing the disulfide. The comparison with the structure of the pig-gluconeogenic FBPase active site provides the same kind of information as well. When these active sites are superimposed, most critical catalytic residues occupy similar positions, with the exception of Glu105 (Glu97 in the pig enzyme), the ligand of the catalytic Mg ions. This residue is pushed away from the active site, as a consequence of the displacement of two beta-strands of the N-terminal beta-sheet, which makes the active site dysfunctional for the catalytic Mg ions. This observation explains why, by strongly increasing the Mg ion concentration in the reaction medium, the catalytic activity can be 'rescued' and made redox-independent. The reduction of the disulfide destabilizes the insertion and releases the beta strands, allowing the active site to reach a catalytically favorable conformation. The conclusions drawn from the structural analyses are corroborated by studies of the Mg^{2+} dependency of the activity of oxidized, reduced and mutant FBPases, which show that the opening of the regulatory disulfide, either by reduction or mutation, decreases the $S_{0.5}$ for Mg^{2+} by a factor of 20 to the same low value (Balmer et al. 2001).

Chloroplastic FBPase exhibits strict specificity for Trx-*f* as has recently been reconfirmed with the two isoforms of Trx-*f*, which are present in *Arabidopsis* chloroplasts (Collin et al. 2003).

The regulatory disulfide of FBPase has a somewhat more negative redox potential than Trx-*f* (Balmer et al. 2001), however, the difference in potential is smaller than what is observed for the C-terminal disulfide of NADP-MDH. This nevertheless means that for full activation of FBPase an excess of reduced Trx-*f* has to be present in the stroma.

A detailed survey of the catalytical properties of chloroplast FBPases has been published recently (Chueca et al. 2002).

Glyceraldehyde-3 phosphate dehydrogenase

The photosynthetic GAPDH is another Calvin-cycle enzyme belonging to a wide group of GAPDHs found in most organisms displaying oxygenic photosynthesis. GAPDH catalyze the reaction where glyceraldehyde-3 phosphate is converted into 1,3-bisphosphoglycerate. There are two chloroplastic forms of this enzyme which both are tetrameric and composed of two kinds of subunits: A- and B-subunits.

The subunits are assembled into two different isoforms of this photosynthetic enzyme, having either A4 or A_nB_n stoichiometry. The minor A4 variant has been defined as non-regulatory (Scagliarini et al. 1998), and is thus constitutively active, as opposed to the major regulatory (A_nB_n) isoform. The association behavior and activity of this AB isoform is redox-regulated by Trx-*f*. In addition, regulation by the protein factor CP12 as well as by NAD and 1,3-bisphosphoglycerate

Figure 6 The dimeric NADP-dependent MDH from *Flaveria bidentis* (Carr et al. 1999). The two subunits are in lilac and yellow. In red are the N- and C-terminal extensions, specific for all chloroplastic NADP-MDHs. In each of the extensions is one regulatory disulfide bridge present. The N-terminal extensions (top and bottom) are sitting like wedges between the subunits, thereby locking the domains relative to each other. The C-terminal extensions (at the left and right side of the molecule) are folding back into the active sites and the disulfides stabilize this conformation. The very C-termini are interacting with residues of the active site and with the $NADP^+$.

Figure 7 Oxidized tetrameric pea chloroplastic FBPase (Chiadmi et al. 1999). The disulfide between Cys153 and Cys173 is shown.

Figure 8 The three-dimensional structure of the constitutively active A4 tetramer of photosynthetic glyceraldehyde-3-phosphate dehydrogenase (GAPDH) of *Spinacia oleracea* (Fermani et al. 2001; Falini et al. 2003).

has also been reported (Wedel and Soll 1998; Lebreton and Gontero 1999; Lebreton et al. 2003). These factors have an effect on the oligomerization state of the enzyme and on its association with phophoribulokinase, another Calvin-cycle enzyme.

A catalytic difference with respect to glycolytic GAPDH, is that photosynthetic GAPDH exhibits dual cofactor specificity toward pyridine nucleotides with a preference for NADP(H) (Falini et al. 2003). The enzyme is thus able to use either NADH or NADPH as a cofactor, but only the NADPH-dependent activity is redox-regulated.

The B-subunits, 80% homologous to A-subunits, display a 28 amino-acid residue long C-terminal extension bearing two conserved cysteines that have been shown to be implicated in the redox regulation, where the C-terminal extension acts as an autoinhibitory domain regulated by thioredoxin and NAD (Qi et al. 2001; Sparla et al. 2002).

The three-dimensional structure of the constitutively active A4 tetramer has been solved with two different cofactors NADP and NAD (Fermani et al. 2001; Falini et al. 2003). The overall structure is very similar to that of other known glycolytic GAPDH structures (Figure 8). As this A4 structure lacks the regulatory extensions and there is so far no structure available for the redox-regulated form, we still have no proof of how the redox regulation takes place in detail.

Conclusions

The striking feature of the thioredoxin-regulated enzymes for which structures are available, is that the regulatory disulfides are distant from the active site but their oxido-reduction state triggers conformational changes having direct consequences on the active-site structure. The structural data are then very important to fully understand the intramolecular modifications linked to activation. There are only few three-dimensional structures available so far for thioredoxin-regulated enzymes and more structures are needed to fully understand how the thioredoxin affects its targets.

References

Antonkine ML, Jordan P, Fromme P, Krauss N, Golbeck JH and Stehlik D (2003) Assembly of protein subunits within the stromal ridge of Photosystem I. Structural changes between unbound and sequentially PS I-bound polypeptides and correlated changes of the magnetic properties of the terminal iron sulfur clusters. J Mol Biol 327: 671–697

Balmer Y and Schürmann P (2001) Heterodimer formation between thioredoxin *f* and fructose 1,6-bisphosphatase from spinach chloroplasts. FEBS Lett 492: 58–61

Balmer Y, Stritt-Etter A-L, Hirasawa M, Jacquot J-P, Keryer E, Knaff DB and Schürmann P (2001) Oxidation-reduction and activation properties of chloroplast fructose 1,6-bisphosphatase with mutated regulatory site. Biochemistry 40: 15444–15450

Balmer Y, Koller A, del Val G, Manieri W, Schürmann P and Buchanan BB (2003) Proteomics gives insight into the regulatory function of chloroplast thioredoxins. Proc Natl Acad Sci USA 100: 370–375

Barber J and Andersson B (1994) Revealing the blueprint of photosynthesis. Nature 370: 31–34

Brandes H, Larimer F and Hartman F (1996) The molecular pathway for the regulation of phosphoribulokinase by thioredoxin *f*. J Biol Chem 271: 3333–3335

Buchanan BB (1992) Carbon dioxide assimilation in oxygenic and anoxygenic photosynthesis. Photosynth Res 33: 147–162

Buchanan B, Schürmann P, Wolosiuk R and Jacquot J (2002) The ferredoxin/thioredoxin system: from discovery to molecular structures and beyond. Photosynth Res 73: 215–222

Capitani G, Markovic-Housley Z, DelVal G, Morris M, Jansonius JN and Schürmann P (2000) Crystal structures of two functionally different thioredoxins in spinach chloroplasts. J Mol Biol 302: 135–154

Carr PD, Verger D, Ashton AR and Ollis DL (1999) Chloroplast NADP-malate dehydrogenase: structural basis of light-dependent regulation of activity by thiol oxidation and reduction. Structure 7: 461–475

Chiadmi M, Navaza A, Miginiac-Maslow M, Jacquot JP and Cherfils J (1999) Redox signalling in the chloroplast: structure of oxidized pea fructose-1,6-bisphosphate phosphatase. EMBO J 18: 6809–5815

Chueca A, Sahrawy M, Pagano EA and Lopêz-Gorge J (2002) Chloroplast fructose-1,6-bisphosphatase: structure and function. Photosynth Res 75: 235–249

Collin V, Issakidis-Bourguet E, Marchand C, Hirasawa M, Lancelin JM, Knaff DB and Miginiac-Maslow M (2003) The Arabidopsis plastidial thioredoxins: new functions and new insights into specificity. J Biol Chem 278: 23747–23752

Dai S, Saarinen M, Ramaswamy S, Meyer Y, Jacquot JP and Eklund H (1996) Crystal structure of *Arabidopsis thaliana* NADPH dependent thioredoxin reductase at 2.5 Å resolution. J Mol Biol 264: 1044–1057

Dai S, Schwendtmayer C, Schürmann P, Ramaswamy S and Eklund H (2000) Redox signaling in chloroplasts: cleavage of disulfides by an iron-sulfur cluster. Science 287: 655–658

De Pascalis AR, Schurmann P and Bosshard HR (1994). Comparison of the binding sites of plant ferredoxin for two ferredoxin-dependent enzymes. FEBS Lett 337: 217–220

del Val G, Maurer F, Stutz E and Schürmann P (1999) Modification of the reactivity of spinach chloroplast thioredoxin *f* by site-directed mutagenesis. Plant Sci 149: 183–190

Falini G, Fermani S, Ripamonti A, Sabatino P, Sparla F, Pupillo P and Trost P (2003) Dual coenzyme specificity of photosynthetic glyceraldehyde-3-phosphate dehydrogenase interpreted by the crystal structure of A4 isoform complexed with NAD. Biochemistry 42: 4631–4639

Fermani S, Ripamonti A, Sabatino P, Zanotti G, Scagliarini S, Sparla F, Trost P and Pupillo P (2001) Crystal structure of the non-regulatory A(4) isoform of spinach chloroplast glyceraldehyde-3-phosphate dehydrogenase complexed with NADP. J Mol Biol 314: 527–542

Gomez I, Merchan F, Fernandez E and Quesada A (2002) NADP-malate dehydrogenase from *Chlamydomonas*: prediction of new

structural determinants for redox regulation by homology modeling. Plant Mol Biol 48: 211–221

Goyer A, Decottignies P, Lemaire S, Ruelland E, Issakidis-Bourguet E, Jacquot J-P and Miginiac-Maslow M (1999) The internal Cys207 of sorghum leaf NADP-malate dehydrogenase can form mixed disulfides with thioredoxin. FEBS Lett 444: 165–169

Goyer A, Decottignies P, Issakidis-Bourguet E and Miginiac-Maslow M (2001) Sites of interaction of thioredoxin with sorghum NADP-malate dehydrogenase. FEBS Lett 505: 405–408

Hatch MD (1987) C4 photosynthesis: a unique blend of modified biochemistry, anatomy and ultrastructure. Biochim Biophys Acta 895: 81–106

Hirasawa M, Schürmann P, Jacquot J-P, Manieri W, Jacquot P, Keryer E, Hartman FC and Knaff DB (1999) Oxidation–reduction properties of chloroplast thioredoxins, ferredoxin:thioredoxin reductase and thioredoxin *f*-regulated enzymes. Biochemistry 38: 5200–5205

Hirasawa M, Ruelland E, Schepens I, Issakidis-Bourguet E, Miginiac-Maslow M and Knaff DB (2000) Oxidation–reduction properties of the regulatory disulfides of sorghum chloroplast nicotinamide adenine dinucleotide phosphate-malate dehydrogenase. Biochemistry 39: 3344–3350

Issakidis E, Miginiac-Maslow M, Decottignies P, Jacquot JP, Cretin C and Gadal P (1992) Site-directed mutagenesis reveals the involvement of an additional thioredoxin-dependent regulatory site in the activation of recombinant sorghum leaf NADP-malate dehydrogenase. J Biol Chem 267: 21577–21683

Issakidis E, Saarinen M, Decottignies P, Jacquot J-P, Crétin C, Gadal P and Miginiac-Maslow M (1994) Identification and characterization of the second regulatory disulfide bridge of recombinant sorghum leaf NADP-malate dehydrogenase. J Biol Chem 269: 3511–3517

Issakidis E, Lemaire M, Decottignies P, Jacquot JP and Miginiac-Maslow M (1996) Direct evidence for the different roles of the N- and C-terminal regulatory disulfides of sorghum leaf NADP-malate dehydrogenase in its activation by reduced thioredoxin. FEBS Lett 392: 121–124

Jacquot JP, Lopez-Jaramillo J, Miginiac-Maslow M, Lemaire S, Cherfils J, Chueca A and Lopez-Gorge J (1997a) Cysteine-153 is required for redox regulation of pea chloroplast fructose-1,6-bisphosphatase. FEBS Lett 401: 143–147

Jacquot J-P, Lancelin J-M and Meyer Y (1997b) Thioredoxins: structure and function in plant cells. New Phytol 136: 543–570

Jameson GN, Walters EM, Manieri W, Schürmann P, Johnson MK and Huynh BH (2003) Spectroscopic evidence for site specific chemistry at a unique iron site of the [4Fe–4S] cluster in ferredoxin:thioredoxin reductase. J Am Chem Soc 125: 1146–1147

Johansson K, Ramaswamy S, Saarinen M, Lemaire-Chamley M, Issakidis-Bourguet E, Miginiac-Maslow M and Eklund H (1999) Structural basis for light activation of a chloroplast enzyme: the structure of sorghum NADP-malate dehydrogenase in its oxidized form. Biochemistry 38: 4319–4326

Knaff DB (1996) Ferredoxin and ferredoxin-dependent enzymes. In: Yocum CF and Ort DR (eds) Advances in Photosynthesis, pp 333–361. Kluwer Academic Publishers, Dordrecht, The Netherlands

Kobe B and Kemp BE (1999) Active site-directed protein regulation. Nature 402: 373–376

Krimm I, Goyer A, Issakidis-Bourguet E, Miginiac-Maslow M and Lancelin JM (1999) Direct NMR observation of the thioredoxin-mediated reduction of the chloroplast NADP-malate dehydrogenase provides a structural basis for the relief of autoinhibition. J Biol Chem 274: 34539–34542

Lebreton S and Gontero B (1999) Memory and imprinting in multienzyme complexes. Evidence for information transfer from glyceraldehyde-3-phosphate dehydrogenase to phosphoribulokinase under reduced state in *Chlamydomonas reinhardtii*. J Biol Chem 274: 20879–20884

Lebreton S, Graciet E and Gontero B (2003) Modulation, via protein–protein interactions, of glyceraldehyde-3-phosphate dehydrogenase activity through redox phosphoribulokinase regulation. J Biol Chem 278: 12078–12084

Lemaire M, Schmitter JM, Issakidis E, Miginiac-Maslow M, Gadal P and Decottignies P (1994) Essential histidine at the active site of sorghum leaf NADP-dependent malate dehydrogenase. J Biol Chem 269: 27291–27296

Lemaire SD, Collin V, Keryer E, Quesada A and Miginiac-Maslow M (2003) Characterization of thioredoxin *y*, a new type of thioredoxin identified in the genome of *Chlamydomonas reinhardtii*. FEBS Lett 543: 87–92

Manieri W, Franchini L, Raeber L, Dai S, Stritt-Etter A-L and Schürmann P (2003) N-terminal truncation of the variable subunit stabilizes spinach ferredoxin:thioredoxin reductase. FEBS Lett 549: 167–170

Meyer Y, Vignols F and Reicheld J-P (2002) Classification of plant thioredoxins by sequence similarity and intron position. Meth Enzymol 347: 394–402

Miginiac-Maslow M and Lancelin J-M (2002) Intrasteric inhibition in redox signalling: light activation of NADP-malate dehydrogenase. Photosynth Res 72: 1–12

Miginiac-Maslow M, Decottignies P, Jacquot J-P and Gadal P (1990) Regulation of corn leaf NADP-malate dehydrogenase light-activation by the photosynthetic electron flow. Effect of photoinhibition studied in a reconstituted system. Biochim Biophys Acta Bio-Energetics 1017: 273–279

Miginiac-Maslow M, Issakidis E, Lemaire M, Ruelland E, Jacquot JP and Decottignies P (1997) Light-dependent activation of NADP-malate dehydrogenase: a complex process. Aust J Plant Physiol 24: 529–542

Motohashi K, Kondoh A, Stumpp MT and Hisabori T (2001) Comprehensive survey of proteins targeted by chloroplast thioredoxin. Proc Natl Acad Sci USA 98: 11224–11229

Ocheretina O, Haferkamp I, Tellioglu H and Scheibe R (2000) Light-modulated NADP-malate dehydrogenases from mossfern and green algae: insights into evolution of the enzyme's regulation. Gene 258: 147–154

Powis G and Montfort WR (2001) Properties and biological activities of thioredoxins. Annu Rev Biophys Biomol Struct 30: 421–455

Qi J, Isupov M, Littlechild J and Anderson L (2001) Chloroplast glyceraldehyde-3-phosphate dehydrogenase contains a single disulfide bond located in the C-terminal extension to the B subunit. J Biol Chem 276: 35247–35252

Ruelland E and Miginiac-Maslow M (1999) Regulation of chloroplast enzyme activities by thioredoxins: activation or relief from inhibition? Trends Plant Sci 4: 136–141

Ruelland E, Lemaire-Chamley M, Le Marechal P, Issakidis-Bourguet E, Djukic N and Miginiac-Maslow M (1997) An internal cysteine is involved in the thioredoxin-dependent activation of sorghum leaf NADP-malate dehydrogenase. J Biol Chem 272: 19851–19857

Ruelland E, Johansson K, Decottignies P, Djukic N and Miginiac-Maslow M (1998) The autoinhibition of sorghum NADP malate dehydrogenase is mediated by a C-terminal negative charge. J Biol Chem 273: 33482–33488

Saarinen M, Gleason FK and Eklund H (1995). Crystal structure of thioredoxin-2 from Anabaena. Structure 3: 1097–1108

Scagliarini S, Trost P and Pupillo P (1998) The non-regulatory isoform of NADP(H)-glyceraldehyde-3-phosphate dehydrogenase from spinach chloroplasts. J Exp Bot 49: 1307–1315

Schepens I, Johansson K, Decottignies P, Gillibert M, Hirasawa M, Knaff D and Miginiac-Maslow M (2000a) Inhibition of the thioredoxin-dependent activation of the NADP-malate dehydrogenase and cofactor specificity. J Biol Chem 275: 20996–21001

Schepens I, Ruelland E, Miginiac-Maslow M, Le Marechal P and Decottignies P (2000b) The role of active site arginines of sorghum NADP-malate dehydrogenase in thioredoxin-dependent activation and activity. J Biol Chem 275: 35792–35798

Schürmann P (2003) Redox signaling in the chloroplast: the ferredoxin/thioredoxin system. Antioxid Redox Signal 5: 69–78

Schürmann P and Buchanan BB (2001) The structure and function of the ferredoxin/thioredoxin system in photosynthesis. In: Aro E-M and Andersson B (eds) Regulatory Aspects of Photosynthesis. Advances in Photosynthesis, pp 331–361. Kluwer Academic Publishers, Dordrecht, The Netherlands

Schürmann P and Jacquot J (2000) Plant thioredoxin systems revisited. Annu Rev Plant Phys 51: 371–400

Schwendtmayer C, Manieri W, Hirasawa M, Knaff DB and Schürmann P (1998) Cloning, expression and characterization of ferredoxin:thioredoxin reductase from *Synechocystis* sp. PCC6803. In: Garab G (ed) Photosynthesis: Mechanisms and Effects (Proceedings of the XIth International Congress on Photosynthesis, Budapest, Hungary), pp 1927–1930. Kluwer Academic Publishers, Dordrecht, The Netherlands

Sparla F, Pupillo P and Trost P (2002) The C-terminal extension of glyceraldehyde-3-phosphate dehydrogenase subunit B acts as an autoinhibitory domain regulated by thioredoxins and nicotinamide adenine dinucleotide. J Biol Chem 277: 44946–44952

Staples CR, Ameyibor E, Fu W, Gardet-Salvi L, Stritt-Etter AL, Schürmann P, Knaff DB and Johnson MK (1996) The function and properties of the iron-sulfur center in spinach ferredoxin:thioredoxin reductase: a new biological role for iron-sulfur clusters. Biochemistry 35: 11425–11434

Staples CR, Gaymard E, Stritt-Etter AL, Telser J, Hoffman BM, Schürmann P, Knaff DB and Johnson MK (1998) Role of the $[Fe_4S_4]$ cluster in mediating disulfide reduction in spinach ferredoxin:thioredoxin reductase. Biochemistry 37: 4612–4620

Villeret V, Huang S, Zhang Y, Xue Y and Lipscomb WN (1995) Crystal structure of spinach chloroplast fructose-1,6-bisphosphatase at 2.8 Å resolution. Biochemistry 34: 4299–4306

Wedel N and Soll J (1998) Evolutionary conserved light regulation of Calvin cycle activity by NADPH-mediated reversible phosphoribulokinase/CP12/ glyceraldehyde-3-phosphate dehydrogenase complex dissociation. Proc Natl Acad Sci USA 95: 9699–9704

Williams Jr CH (1992) Lipoaminde dehydrogenase, glutathione reductase, thioredoxin reductase, and mercury ion reductase – a family of flavoenzyme transhydrogenases. In: Müller F (ed) Chemistry and Biochemistry of Flavoenzymes, pp 121–211. CRC Press, Boca Raton, Florida

Wolosiuk RA, Ballicora MA and Hagelin K (1993) The reductive pentose phosphate cycle for photosynthetic CO_2 assimilation: enzyme modulation. FASEB J 7: 622–637